PRAMANA
— journal of
physics

Vol. 58, No. 2
February 2002
pp. 371–383

Arrays of magnetic nanoparticles capped with alkylamines

P JOHN THOMAS, P SARAVANAN, G U KULKARNI and C N R RAO*
Chemistry and Physics of Materials Unit, Jawaharlal Nehru Centre for Advanced Scientific Research, Jakkur, Bangalore 560 064, India
*for correspondence: cnrrao@jncasr.ac.in

Abstract. Magnetic metal and metal oxide nanoparticles capped with alkylamines have been synthesized and characterized by transmission electron microscopy, X-ray diffraction, energy dispersive X-ray analysis and magnetization measurements. Core-shell Pd–Ni particles with composition, $Pd_{561}Ni_{3000}$, (diameter ∼3.3 nm) are superparamagnetic at 5 K and organize themselves into two-dimensional crystalline arrays. Similar arrays are obtained with $Pd_{561}Ni_{3000}Pd_{1500}$ nanoparticles containing an additional Pd shell. Magnetic spinel particles of γ-Fe_2O_3, Fe_3O_4 and $CoFe_2O_4$ of average diameters in the 4–6 nm range coated with octylamine are all supermagnetic at room temperature and yield close-packed disordered arrays. Relatively regular arrays are formed by dodecylamine-capped Fe_3O_4 nanoparticles (∼8.6 nm diameter) while well-ordered hexagonal arrays were obtained with octylamine-covered Co_3O_4 nanoparticles (∼4.2 nm diameter).

Keywords. Self-assembly; magnetic nanoparticles.

PACS Nos 81.16.D; 81.07.Bc; 81.16.B

1. Introduction

Nanoparticles in mesoscopic organizations are attracting attention because of their fascinating properties and potential applications in future technology [1]. For instance, assemblies of magnetic nanoparticles are considered to be of importance in future magnetic recording [2,3]. An important aspect of this area of research relates to the size-dependent electronic and magnetic properties of the nanoparticles themselves [4,5]. Synthesis and programmed assembly of nanoparticles of choice therefore assumes great significance. It has been shown recently that metal or semi-conductor nanoparticles coated with surfactants such as thiols, silanes, phospholipids or phosphines organize spontaneously into primitive superstructures on flat substrates [6]. The key role played by the particle diameter (d) relative to the length of the surfactant chain (l) in determining the structure of such superlattices has been recognized [7].

Two-dimensional arrays of magnetic cobalt nanoparticles exhibiting collective magnetic properties have been reported in the recent literature [8,9]. Arrays of magnetic particles of bimetallic Fe–Pt nanoparticles have been prepared using oleic acid and oleylamine as stabilizers by Sun *et al* [10]. The results of this study suggest that such an assembly can support high-density reversible magnetization. We have been investigating arrays of magnetic Pd–Ni nanoparticles with a core-shell structure prepared by using *n*-alkane thiols as

stabilizers [11]. While there has been reasonable success in preparing arrays of metal and semiconducting chalcoginide nanoparticles, arrays of metal oxides are relatively unknown [12,13]. We considered it important to prepare arrays of metal oxide particles with useful magnetic properties, particularly in view of their stability under ambient conditions. In this report, we examine the arrays of octylamine-coated magnetic Pd–Ni and Pd–Ni–Pd core-shell nanoparticles of the compositions $Pd_{561}Ni_{3000}$ and $Pd_{561}Ni_{3000}Pd_{1500}$, along with those of γ-Fe_2O_3, Co_3O_4, Fe_3O_4, $CoFe_2O_4$ and $MnFe_2O_4$ nanoparticles coated with long-chain amines. The results of this preliminary study are encouraging and suggest that further investigations may indeed be profitable.

2. Experimental

2.1 *Synthesis of Pd–Ni nanoparticles*

Metal nanoparticles are generally prepared by the controlled reduction [14] in the presence of a surfactant. In order to obtain monodisperse magnetic particles of Ni, a magic nuclearity Pd_{561} seed was employed through a two-step process involving a ligand exchange reaction [15,16]. The Ni particles so obtained are protected against oxidation by an outer shell of Pd. Pd_{561} nanoparticles were first obtained by reducing 15 ml of a 2.0 mM aqueous solution of H_2PdCl_4 by refluxing it with a mixture of 15 ml of absolute ethanol and 25 ml of water containing 33.3 mg of PVP ($M_w \sim 40000$ g mol^{-1}) for $\sim$3 h. The solvent was then evaporated and the particles were redispersed in 100 ml of Ar-purged 1-propanol followed by addition of 160 μmol of $Ni(CH_3COO)_2.4H_2O$ and 40 mg of PVP. The mixture was reduced by refluxing under Ar flow for 3 h to obtain $Pd_{561}Ni_{3000}$ particles. The three shell particles, $Pd_{561}Ni_{3000}Pd_{1500}$, were obtained by refluxing with 80 μmol of H_2PdCl_4 (2.0 mM solution) and PVP in ethanol-water mixture. The replacement of the ligand was accomplished based on a method invented in our lab. Accordingly, 2.0 ml aqueous sol containing $Pd_{561}Ni_{3000}Pd_{1500}$ particles was thoroughly mixed with a toluene solution (2 ml) containing *n*-octylamine ($\sim$20 μl) to obtain a miscelle to which a dilute solution of $NaBH_4$ (2 ml of 2 mM solution) was added. This resulted in the separation of the aqueous and the organic layers, with the particles quantitatively transferred to the organic phase. Excess *n*-octylamine could be removed by precipitating the nanoparticles with methanol. Similarly, using concentrated HCl instead of $NaBH_4$ and *n*-octylthiol instead of *n*-octylamine, octanethiol-stabilized Pd–Ni nanoparticles were obtained.

2.2 *Synthesis of oxide nanoparticles*

This was accomplished either by arrested precipitation or by thermal decomposition of organo-metallic precursors under carefully controlled conditions. It has been suggested that metal cupferronates could be used as precursors in the synthesis of metal nanoparticles [17]. Iron, cobalt and manganese cupferronates (cup) were prepared by precipitation by slowly adding aqueous cupferron to aqueous solutions of the respective chlorides [18]. The pH of the solution was maintained at 2.0 for the precipitation of iron cupferronate. The solids were recrystallized from alcohol and were brown, greyish brown and red for Fe,

Mn and Co respectively. The recrystallized cupferronates exhibited characteristic IR bands and were free of unreacted cupferron [18].

Nanoparticles of γ-Fe_2O_3, Fe_3O_4, Co_3O_4, $CoFe_2O_4$ and $MnFe_2O_4$ were prepared by thermal decomposition of the metal cupferronates. In a typical synthesis yielding γ-Fe_2O_3 nanoparticles, a 0.3 mM solution of the $Fe(cup)_3$ in *n*-octylamine was injected into a vigorously stirred 9 mL solution of tri-*n*-octylamine at $\sim$300 °C in a round bottomed flask. The onset of reduction was marked by change in color from red-brown to brown-black with brisk effervescence. The contents of the flask were maintained at $\sim$225 °C and the stirring continued for another 45 min. To obtain Fe_3O_4 particles, the decomposition of cupferronates was carried out in H_2 atmosphere and the contents of the flask were maintained at $\sim$250°C till a color change from brown to black was observed. Co_3O_4 nanoparticles were prepared starting from $Co(cup)_2$. A 1:2 mixture of Co and Fe cupferronates yielded $CoFe_2O_4$ nanoparticles. Similarly, a 1:2 mixture of Mn and Fe cupferronates yielded $MnFe_2O_4$. All the nanoparticles obtained were freely soluble in toluene and could be precipitated (reversibly) using methanol.

The nanoparticles were characterized by several techniques. Energy dispersive X-ray analysis (EDAX) was performed using Links (ISIS) Si(Li) detector of Oxford instruments fitted to a Lieca S-440i scanning electron microscope. Samples were prepared by depositing a drop of the toluene sol on Al stub. Transmission electron microscopy (TEM) and selected area electron diffraction (SAED) measurements were performed with a 300 kV JEOL 3010 transmission electron microscope. Samples for TEM were prepared by depositing a drop of the toluene sol on a holey copper carbon grid and allowing it to dry in a dessicator overnight. X-ray diffraction measurements were performed using Seifart 3000 X-ray powder diffractometer equipped with Cu-Kα radiation source employing 0.02 ° step size. Magnetic measurements were carried out on dry powder samples using vibrating sample magnetometer equipped with a superconducting magnet capable of reaching fields up to 50 kOe and temperatures down to 5 K.

3. Results and discussion

3.1 *Pd–Ni nanoparticles*

EDAX analysis of the Pd–Ni particles yielded Pd:Ni ratios of 0.837 and 0.727 in the case of $Pd_{561}Ni_{3000}$ and $Pd_{561}Ni_{3000}Pd_{1500}$ respectively, in agreement with the expected values of 0.842 and 0.695. In figure 1, we present typical TEM micrographs of *n*-octylamine and *n*-octanethiol covered $Pd_{561}Ni_{3000}$ nanoparticles. In both the cases, we observe particles with a uniform diameter of $\sim$3.3 nm arranged in well-ordered arrays extending over a few microns. Importantly, we find no observable change in the size or composition of the particles upon ligand replacement either with thiol or with amine. In the case of octylamine (figure 1a), we observe an hexagonal array with the nearest neighbor spacing (surface to surface) of $\sim$1.7 nm. Assuming that octylamine is present in the fully extended all-trans conformation inclined at 30° to the nanocrystal surface [19], an interparticle spacing of 2.4 nm is expected. The observed spacing suggests that the chains may penetrate into each other up to 30%. Interdigation values of up to 35% have been observed earlier in the case of Pd nanocrystals covered with alkane thiols [7]. Thiol coating, on the other hand, results in multi-layered structures in the form of tapes and wires (figure 1b). It is interesting to

note that a change in the head group of the surfactant from a thiol to an amine brings about a pronounced change in the nature of the organization, even though the chain length is identical.

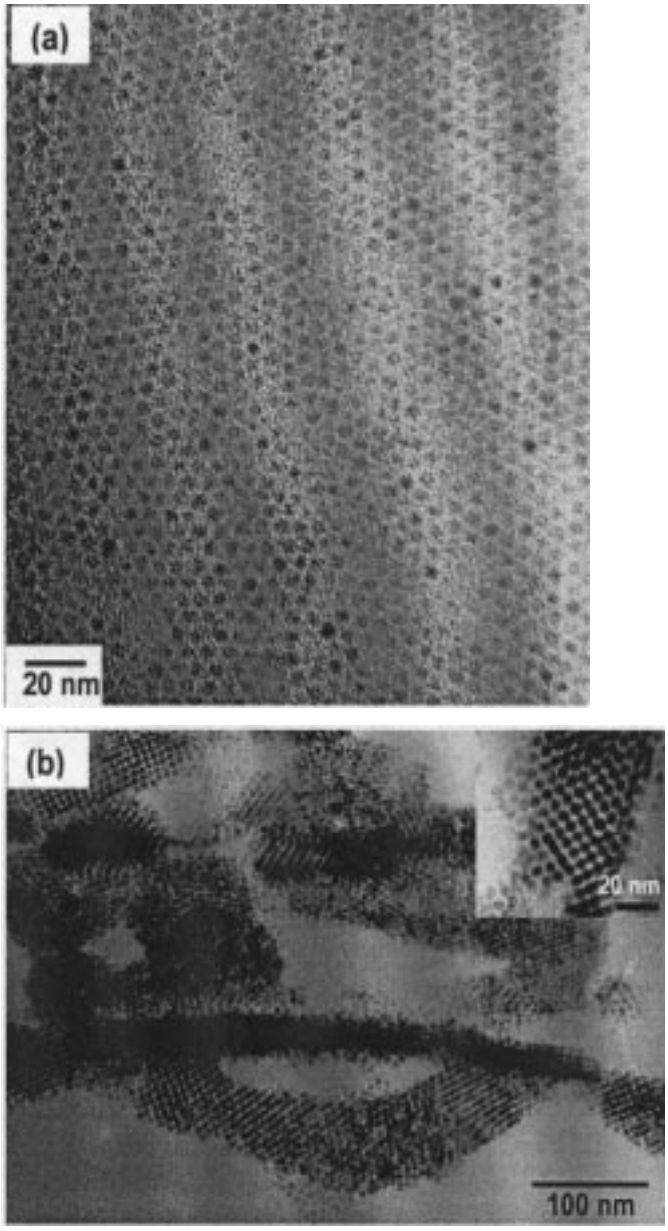

Figure 1. TEM micrograph showing arrays of $Pd_{561}Ni_{3000}$ nanoparticles coated with (**a**) octylamine and (**b**) octanethiol.

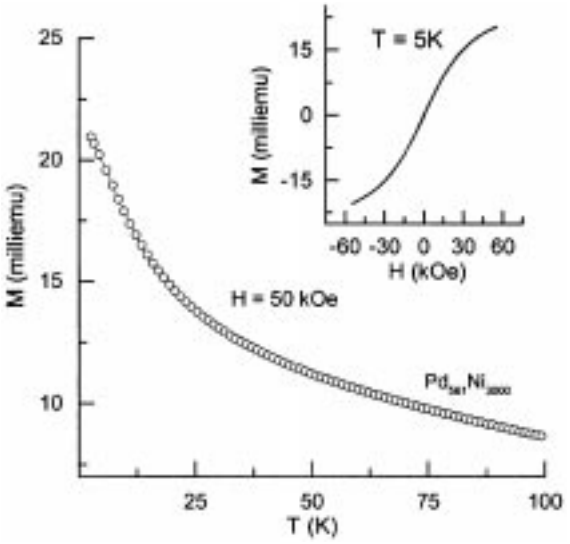

Figure 2. Temperature dependence of the magnetization of $Pd_{561}Ni_{3000}$ core-shell nanoparticles capped with octanethiol under an applied field of 50 kOe. The values were corrected for the contribution from the solvent and the glass tube. Inset shows the change in the magnetization (uncorrected) as a function of magnetic field.

Magnetic measurements were carried out on a toluene dispersion of $Pd_{561}Ni_{3000}$ nanoparticles sealed in a glass tube. The zero-field cooled (ZFC) measurements for octanethiol coated particles are shown in figure 2. However, the field-cooled measurements ($H = 50$ kOe) yield a curve exactly overlapping with the ZFC curve. This implies that the individual moments remain randomized in spite of high magnetic field and low temperature characteristic of a superparamagnetic system with a blocking temperature below 5 K. This is an unusually low blocking temperature for particles of diameter 3.3 nm [20]. Accordingly, these particles do not exhibit a hysteresis even at 5 K as can be seen in the inset of figure 2.

In the core-shell particles of the kind $Pd_{561}Ni_{3000}Pd_{1500}$ described earlier, the outer layer of Pd bequeaths stability to the inner Ni shell. A typical TEM image of octylamine-passivated $Pd_{561}Ni_{3000}Pd_{1500}$ nanoparticles is shown in figure 3. It can be seen that the nanoparticles have an average diameter of 5.5 nm and self-assemble into an extended hexagonal lattice with a typical surface-to-surface interparticle spacing of 1.8 nm corresponding to 25% interdigation.

3.2 *Metal oxide nanoparticles*

The X-ray diffraction pattern of γ-Fe_2O_3 nanoparticles coated with octylamine (figure 4a) shows reflections due to the (220), (311), (400), (511) and (440) planes with the characteristic *d*-spacings of 2.930, 2.490, 2.060, 1.590, 1.464 Å [21] thereby establishing the monophasic nature of the oxide. We have estimated the particle diameter based on the

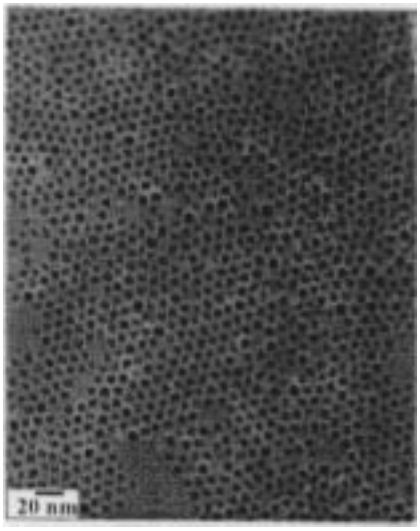

Figure 3. TEM micrograph showing arrays of $Pd_{561}Ni_{3000}Pd_{1500}$ nanoparticles coated with octylamine.

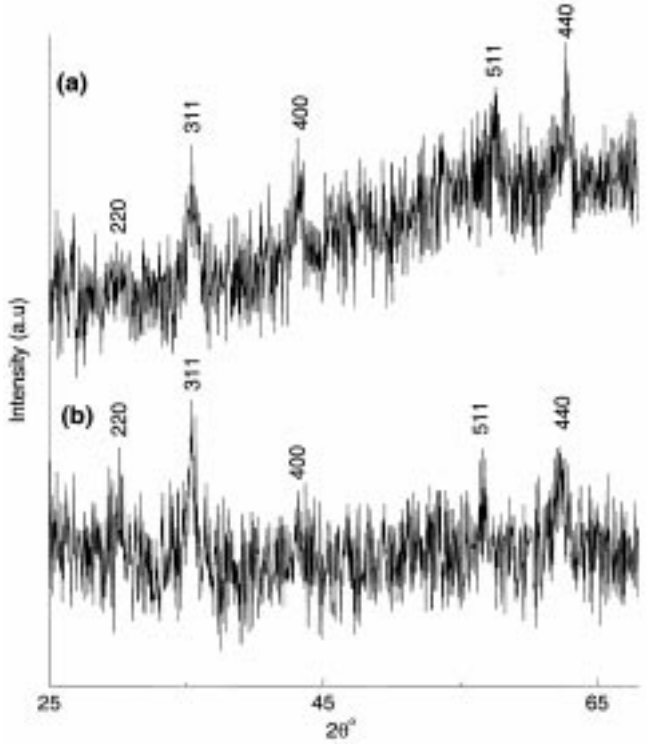

Figure 4. X-ray diffraction patterns of (**a**) γ-Fe_2O_3 and (**b**) Fe_3O_4 nanoparticles.

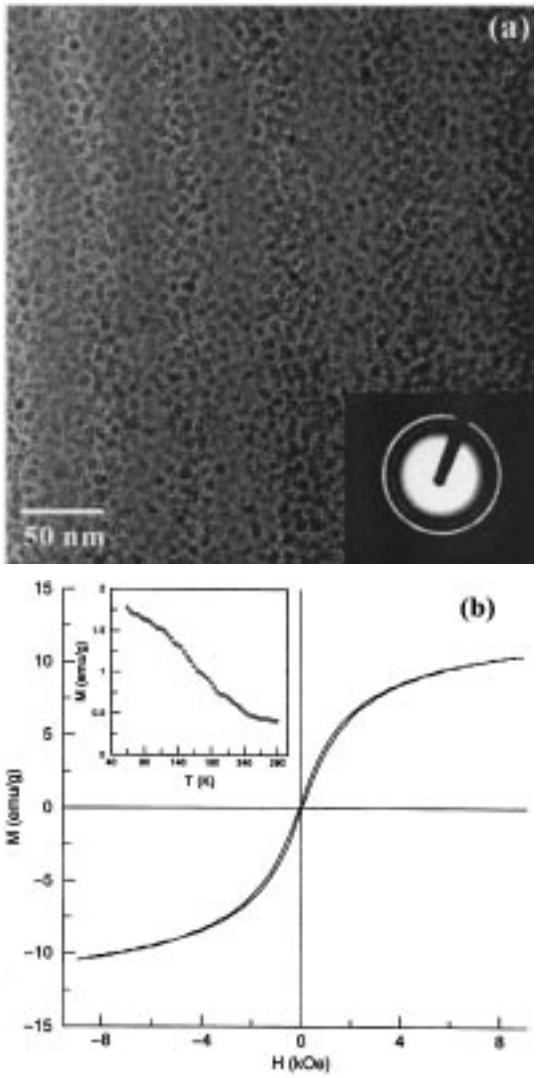

Figure 5. (**a**) TEM micrograph of γ-Fe_2O_3 nanoparticles capped with octylamine. Inset shows the obtained SAED pattern. (**b**) Hysteresis loop exhibited by the γ-Fe_2O_3 nanoparticles. Inset shows the temperature dependence of the paramagnetic moment (under a field of 0.5 kOe).

broadening of the X-ray peaks using the Debye–Scherrer formula [22] to be $\sim$5.9 nm. The TEM image of nearly monodisperse γ-Fe_2O_3 nanoparticles coated with octylamine in figure 5a reveals the presence of nanoparticles with an average diameter of 4.8 nm, which compares well with the diameter determined by XRD. The random close-packed arrangement seen in the image resembles that of jammed arrangements of polydisperse spheroids [23]. The SAED pattern in the inset of figure 5a gives the *d*-spacings consistent

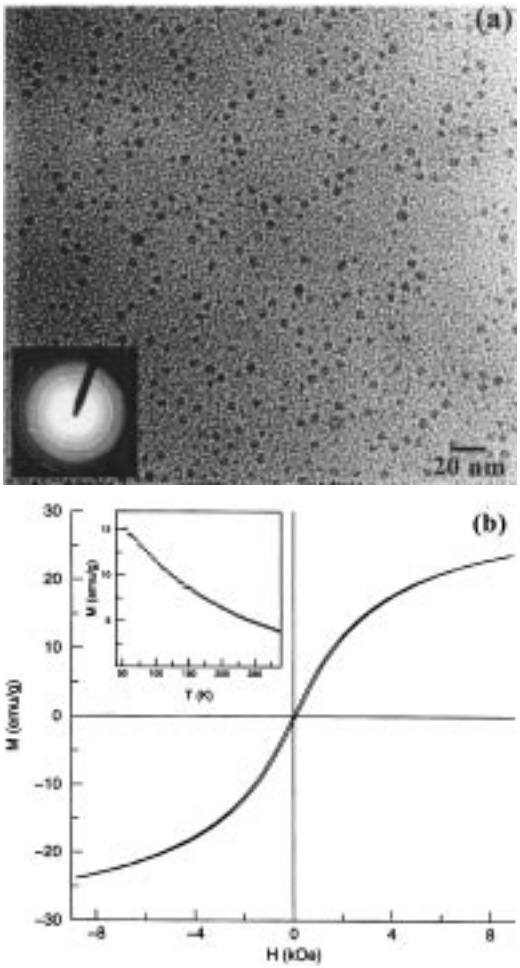

Figure 6. (**a**) TEM micrograph showing Fe_3O_4 nanoparticles capped with octylamine. Inset shows the SAED pattern. (**b**) Hysteresis loop exhibited by the Fe_3O_4 nanoparticles. Inset shows the temperature dependence of the paramagnetic moment (under a field of 0.5 kOe).

with those obtained from X-ray diffraction. Magnetic hysteresis exhibited by the γ-Fe_2O_3 particles at room temperature is shown in figure 5b, with the temperature dependence of magnetization in the inset. The hysteresis loop has a small area (coercivity $\sim$38.1 Oe) with a poor saturation due to the superparamagnetic nature of the particles. The magnetization measurements indicate a strong temperature dependence of the paramagnetic moment. The observed saturation magnetization (M_s) of 10.45 emu/g at 10 kOe is noticeably smaller than the bulk value (73.5 emu/g). The significantly lower M_s and the coercivity value are attributed to the existence of a magnetically inactive surface layer and some diamagnetic contribution from the ligand shell [24,25].

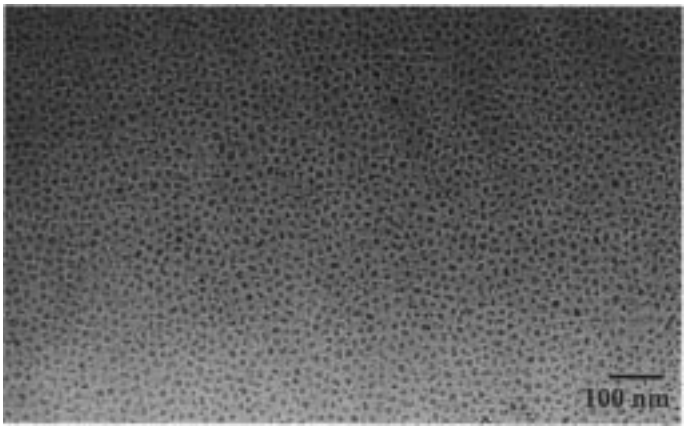

Figure 7. TEM micrograph showing Fe_3O_4 nanoparticles capped with dodecylamine.

The X-ray diffraction pattern of octylamine-coated Fe_3O_4 particles exhibit (figure 4b) peaks at 2.960, 2.530, 2.098, 1.612, 1.471 Å characteristic of monophasic Fe_3O_4 [21]. A typical TEM micrograph of the particles along with the SAED pattern (in the inset) is shown in figure 6a. Isolated particles with an average diameter of 5.0 nm are seen in the imaged region. The diameter estimated from X-ray linewidths is ∼5.8 nm. A saturation magnetization (M_s) of 24.85 emu/g was obtained from the hysteresis loop shown in figure 6b. This is around one fourth of the bulk value for magnetite (92 emu/g). The inset in figure 6b reveals strong temperature dependence of magnetization of the Fe_3O_4 particles. In contrast to the isolated particles obtained with *n*-octylamine, *n*-dodecylamine-capped Fe_3O_4 nanoparticles exhibit a tendency to form close-packed arrays as can be seen from the TEM image in figure 7. The average diameter of particles is ∼8.6 nm.

We have also prepared arrays of non-magnetic Co_3O_4 particles capped with *n*-octylamine. In this case, however, we observe an extended two-dimensional array (figure 8) which is well-ordered. The particles in the hexagonal array have an average diameter of ∼4.2 nm, with a near constant interparticle distance of ∼2.0 nm. In figure 9, we compare the distribution of the nearest neighbour distance in the Co_3O_4 array with that in the Fe_3O_4 array in figure 7. While the interparticle distance is nearly a constant in the case of Co_3O_4 (figure 9a), with 90% of the particles exhibiting a separation of 2.0 nm (corresponding to 17% interdigation of the ligand chain), there is a strong preference for an interparticle separation of 3.2 nm (corresponding to ∼6% interdigation of the amine chains) in the case of Fe_3O_4 particles (figure 9b). Interestingly, the arrangement of the particles of Fe_3O_4 seen in figure 7 resembles the structures obtained at the extrema of the d/l ratio in our study of Pd nanoparticles [7].

Since Co and Mn oxide spinels are ferrimagnetic, they are good candidates for preparing magnetic arrays. EDAX studies of the $CoFe_2O_4$ and $MnFe_2O_4$ nanoparticles yielded Co(Mn) : Fe ratios of 2.2 and 1.9, close to the expected value of 2.00. The X-ray diffraction patterns revealed the monophasic nature of the samples and the spinel structure. The diameters of $CoFe_2O_4$ and $MnFe_2O_4$ nanoparticles were in the ranges of 3–6 nm and 2–5 nm respectively. The TEM micrograph of $CoFe_2O_4$ nanoparticles coated with ocytlamine (figure 10a) shows that these spinel particles organize into a hexagonal lattice over small

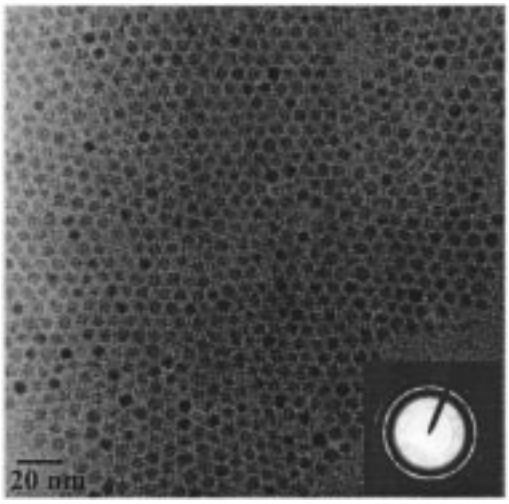

Figure 8. TEM micrograph showing arrays of Co_3O_4 nanoparticles capped with octylamine. Inset shows the SAED pattern.

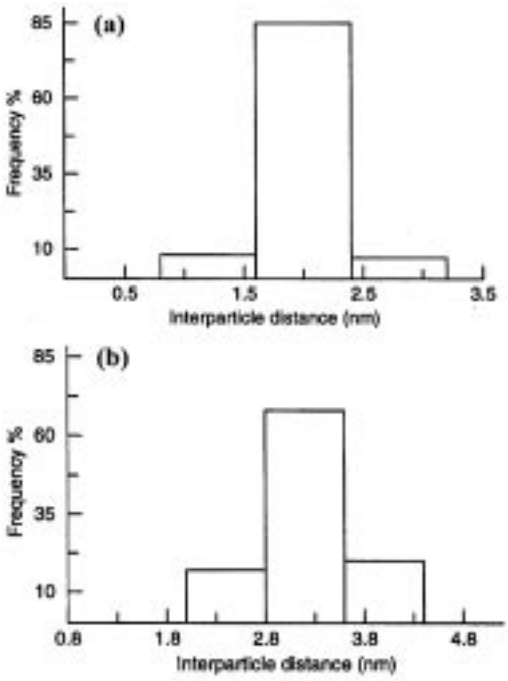

Figure 9. Histograms showing the distribution of interparticle distance in the arrays of (**a**) Co_3O_4 nanoparticles capped with octylamine and (**b**) Fe_3O_4 nanoparticles capped with dodecylamine.

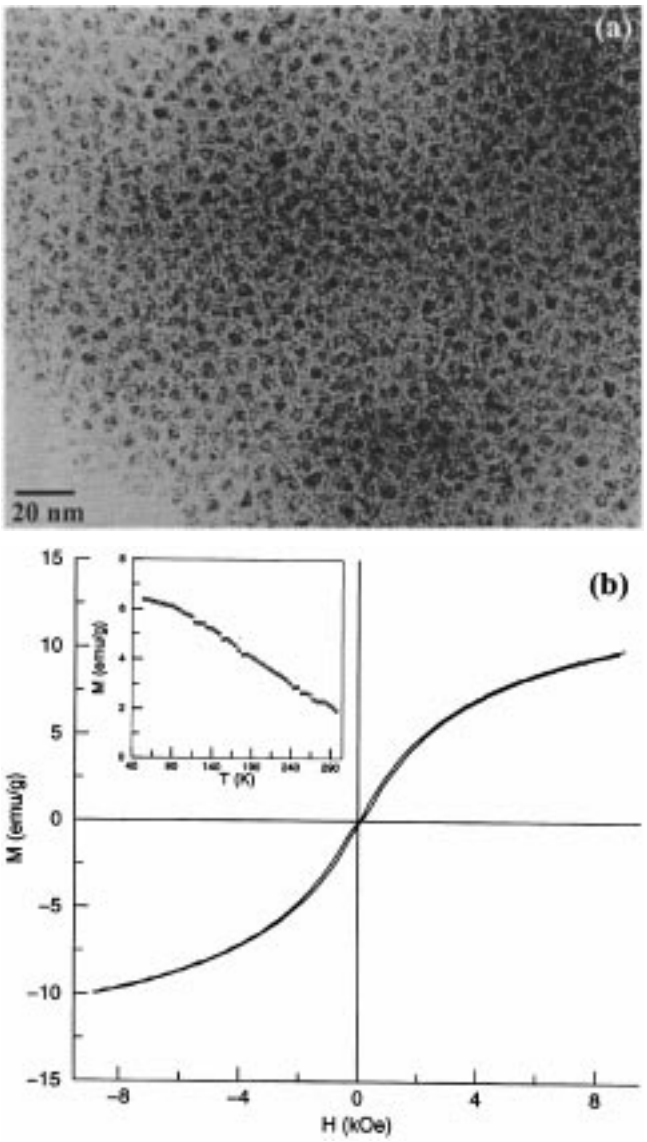

Figure 10. (**a**) TEM micrograph showing $CoFe_2O_4$ nanoparticles capped with octylamine and (**b**) hysteresis loop exhibited by $CoFe_2O_4$ nanoparticles.

regions. The hysteresis loop in figure 10b reveals that the magnetization does not attain saturation up to 10 kOe. The magnetization at this field is ∼10 emu/g which is much lower than the bulk value (∼80 emu/g). Similar results were obtained with the $MnFe_2O_4$ nanoparticles as well.

4. Conclusions

$Pd_{561}Ni_{3000}$ and $Pd_{561}Ni_{3000}Pd_{1500}$ core-shell nanoparticles coated with *n*-octylamine self-assemble yielding good crystalline two-dimensional arrays. The structure of the $Pd_{561}Ni_{3000}$ array depends on the nature of the head group of the surfactant, with the amine yielding an hexagonal two-dimensional array in contrast with the multilayered tapes or wires obtained with the thiol. Octylamine-capped γ-Fe_2O_3 nanoparticles with a superparamagnetic behavior assemble into a jammed array. Relatively regular arrays are obtained with Fe_3O_4 nanoparticles capped with dodecylamine, in contrast with those capped with octylamine. Octylamine capped Co_3O_4 nanoparticles, however, yield good two-dimensional arrays extending to a few microns. The Co and Mn spinel nanoparticles coated with octylamine are superparamagnetic at room temperature and exhibit small scale organization.

Acknowledgement

We thank DRDO for support. One of us (PS) thanks Defence Materials and Stores Research and Development Establishment, Kanpur, for leave of absence.

References

[1] *Nanoparticles and nanostructured films preparation, characterization and applications* edited by J H Fendler (Wiley-VCH, Weinheim, 1998)
[2] S A Majetich and Y Jin, *Science* **284**, 470 (1999)
[3] C H Back, R Allenspach, W Weber, S S P Parkin, D Weller, E L Garwin and H C S Siegmann, *Science* **285**, 864 (1999)
[4] P P Edwards, R L Johnston and C N R Rao in *Metal clusters in chemistry* edited by P Braunstein, G Oro and P R Raithby (Wiely-VCH, New York, 2000)
[5] *Physics and chemistry of small clusters* edited by P Jena, B K Rao and S N Khanna (Plenum Press, New York, 1987)
[6] C N R Rao, G U Kulkarni, P J Thomas and P P Edwards, *Chem. Soc. Rev.* **29**, 27 (2000)
[7] P J Thomas, G U Kulkarni and C N R Rao, *J. Phys. Chem.* **B104**, 8138 (2000)
[8] S Sun and C B Murray, *J. Appl. Phys.* **85**, 4325 (1999)
[9] C Petit and M P Pileni, *Appl. Surf. Sci.* **162–163**, 519 (2000)
[10] S Sun, C B Murray, D Weller, L Folks and A Moser, *Science* **287**, 1989 (2000)
[11] P J Thomas, G U Kulkarni and C N R Rao, *J. Nanosci. Nanotechnol.* **1**, 267 (2001)
[12] M D Bentzon, J V Wonterghem, S Mörup, A Thölén and C J W Koch, *Philos. Mag.* **B60**, 169 (1989)
[13] J S Yin and Z L Wang, *Phys. Rev. Lett.* **79**, 2570 (1997)
[14] *Clusters and Colloids: from theory to applications* edited by G Schmid (Wiley-VCH, Weinheim, 1995)
[15] K V Sarathy, G U Kulkarni and C N R Rao, *Chem. Commun.* 573 (1997)
[16] K V Sarathy, G Raina, R T Yadav, G U Kulkarni and C N R Rao, *J. Phys. Chem.* **B101**, 9876 (1997)
[17] J Rockenberger, E C Scher and A P Alivisatos, *J. Am. Chem. Soc.* **121**, 11590 (1999)
[18] N H Furman, W B Mason and J S Pekola, *Anal. Chem.* **21**, 1325 (1949)

[19] J R Heath, M C Knobler and D V Leff, *J. Phys. Chem.* **B101**, 189 (1997)
[20] R Sappey, E Vincent, N Hadacek, F Chaput, J P Boilot and D Zins, *Phys. Rev.* **B56**, 14551 (1997)
[21] B H Sohn and R E Cohen, *Chem. Mater.* **9**, 264 (1997)
[22] *X-ray diffraction procedures for crystalline and amorphous solids* by H P Klug and L E Alexander (Wiley-Interscience, 1974)
[23] R J Speedy, *J. Phys. Condens. Matter* **10**, 4185 (1998)
[24] M P Morales, S Veintemillas-Verdaguer, M I Montero, C J Serna, A Roig, Li Casas, B Martinez and F Sandiumenge, *Chem. Mater.* **11**, 3058 (1999)
[25] Ò Iglesias and A Labarta, *Phys. Rev.* **B63**, 184416 (2001)